Corneal Wound Repair After Rose Bengal and Green Light Crosslinking: Clinical and Histologic Study

Patricia Gallego-Muñoz,[1] Lucía Ibares-Frías,[1] Elvira Lorenzo,[1] Susana Marcos,[2] Pablo Peréz-Merino,[2] Nandor Bekesi,[2] Irene E. Kochevar,[3] and M. Carmen Martínez-García[1]

[1]Departamento de Biología Celular, Histología y Farmacología, GIR de Técnicas Ópticas para el Diagnóstico, Universidad de Valladolid, Valladolid, Spain
[2]Instituto de Óptica, Consejo Superior de Investigaciones Científicas, Madrid, Spain
[3]Wellman Center for Photomedicine, Massachusetts General Hospital, Harvard Medical School, Boston, Massachusetts, United States

Correspondence: M. Carmen Martínez-García, Departamento de Biología Celular, Histología y Farmacología, Facultad de Medicina, Universidad de Valladolid, C/Ramón y Cajal 7, 47005 Valladolid, Spain; mariacarmen.martinez.garcia@uva.es.

Submitted: December 23, 2016
Accepted: June 1, 2017

Citation: Gallego-Muñoz P, Ibares-Frías L, Lorenzo E, et al. Corneal wound repair after rose bengal and green light crosslinking: clinical and histologic study. *Invest Ophthalmol Vis Sci*. 2017;58:3471–3480. DOI:10.1167/iovs.16-21365

Purpose. To evaluate corneal wound healing after treatment with a new collagen crosslinking protocol using rose bengal dye and green light (RGX).

Methods. One cornea of 20 New Zealand rabbits was de-epithelialized (DE) in an 8-mm diameter circle and, in another group ($n = 25$), the DE corneas were then stained with 0.1% rose bengal for 2 minutes and exposed to green light (532 nm) for 7 minutes (RGX). The contralateral eyes without treatment acted as controls. The animals were clinically followed including fluorescein staining and pachymetry. Healing events were analyzed after euthanasia at 2, 30, and 60 days. Cell death (TUNEL assay), cell proliferation (5-bromo-2′-deoxyuridine incorporation), and cell differentiation to myofibroblasts (α-SMA labeling) were carried out. In addition, loss of keratocytes and subsequent repopulation of the corneal stroma were quantified on hematoxylin-eosin–stained sections.

Results. Wound closure was slower after RGX (4.4 days) then after DE (3.3 days). Cell death was restricted to the anterior central stroma, and the cellular decrease did not differ significantly between RGX and DE corneas. Cell proliferation in the epithelium and stroma appeared at 2 days. In both DE and RGX corneas, recovery of the epithelium was complete at day 30, although cell repopulation of the stroma was not complete at 60 days.

Conclusions. The healing response in corneas after RGX is very similar to that observed after DE alone, suggesting that, along with its short treatment time and limited effect on keratocytes, RGX displays good potential for clinical cornea stiffening.

Keywords: wound repair, crosslinking, keratoconus treatment, rose bengal, cornea

Corneal crosslinking (CXL) is currently used to stiffen the stroma, and thus inhibit the progressive cornea protrusion characteristic of keratoconus and other ectatic corneal diseases.[1–3] This simple and noninvasive technique is based on light-initiated photochemical reactions that induce formation of covalent crosslinks between collagens and between collagen and proteoglycans.[4] A photosensitizer, typically riboflavin (vitamin B2), is applied to the de-epithelialized (DE) cornea, which is then exposed to long wavelength ultraviolet light (370-nm UVA) for up to 30 minutes using the conventional procedure. The photochemical reaction produces reactive oxygen species and radicals that induce formation of covalent bonds.[5] As a result of these reactions, protein crosslinking stabilizes corneal biomechanics and increases corneal stiffness.[6–8]

Thin corneas may not contain enough riboflavin to block the UVA from the endothelium, thus making the procedure unsuitable for these corneas. For this reason, treating corneas thinner than 400 μm after epithelial removal is not recommended.[9] In addition, the conventional and most widely used procedure is lengthy, and a tendency toward progression of keratometry values 24 months after CXL is sometimes reported, particularly among the pediatric population.[10,11]

Alternatives, such as the use of hypo-osmolar riboflavin,[12] transepithelial corneal CXL,[13,14] iontophoresis transcorneal delivery,[15] and accelerated CXL[16,17] have been proposed. However, the safety and efficacy of these procedures is yet to be well established.[18]

For these reasons, new crosslinking techniques are being developed. One new method uses rose bengal (RB) as the photosensitizer together with green light (532 nm) and only requires approximately 10 minutes for treatment. Rose bengal is well known as a diagnostic agent for ocular surface damage. It has already been used with green light to seal corneal wounds without sutures,[19] to attach amniotic membrane to the ocular surface[20] to repair nerves and blood vessels in other tissues and for a clinical study of skin wound sealing.[21]

These studies have shown that RB–green light crosslinking, termed RGX, creates bonds in stromal collagen fibrils similar to the mechanism involved in conventional CXL. Previous ex vivo studies using rabbit eyes have demonstrated that RGX significantly increases corneal stiffness[3] and causes no toxicity to keratocytes 24 hours post treatment.[22] In a recent study of RGX in vivo in rabbit eyes, the green light level that increased corneal stiffness was shown to be safe for the retina, as

evidenced by the lack of damage to the blood–retinal barrier, the retinal photoreceptors, the retinal pigment epithelium, and the choriocapillaris.[23]

In order to further evaluate the safety and effectiveness of the RGX technique a greater understanding of the post-treatment healing process is required; thus, necessitating the use of an experimental animal model. We selected the rabbit because it has been used as a model of corneal wound healing after different surgeries, including conventional crosslinking[24–27] and RGX.[23,24]

The goal of the present study was to characterize the wound healing process after RGX. We compared clinical and histologic outcomes in RGX and DE rabbit eyes in vivo. Eyes were followed for 60 days in order to monitor the healing process.

Materials and Methods

The Animal Ethics Committee at the University of Valladolid approved the animal studies described in this research. Animals were cared for following the guidelines of the ARVO Statement for the Use of Animals in Ophthalmic and Vision Research.

Female adult albino New Zealand rabbits, weighing 2.5 to 3 kg, were supplied by a center listed in the official register as a provider of lab animals (Granja San Francisco, Navarra, Spain).

Treatment Procedure

Forty-five New Zealand white rabbits were divided into two groups. Both were anesthetized with an intramuscular injection of ketamine hydrochloride (37.5 mg/kg, Ketolar; Parke Davis SA, Barcelona, Spain) and xylazine hydrochloride (5 mg/kg, Rompun; Bayer, Leverkusen, Germany) in the thigh, followed by topical application of 0.5% tetracaine hydrochloride and 1 mg of oxybuprocaine (Colircusi Anestésico Doble; Alconcusí SA, Barcelona, Spain).

In one group (20 rabbits), the central corneal epithelium was manually removed by gentle scraping with a sharp scraper in the area of an 8-mm diameter circle demarcated by a trephine (DE group). Contralateral eyes were not DE and were used as controls.

The second group (25 rabbits) was treated with RGX to crosslink corneal proteins. After demarcating a central area with an 8-mm trephine, the epithelial layer was removed. Sterile RB (0.1% in PBS, 0.5 mL) was then dropped onto the cornea and the cornea was exposed to green light. The light source was custom-developed and incorporated a 532-nm laser that delivered an irradiance of 0.25 W/cm^2 (MGL-FN-532; Changchun New Industries, Changchun, China) with a collimating lens that provided an 11-mm Gaussian profile beam at the cornea surface.[3,22]

The RGX protocol involved staining the DE cornea surface for 2 minutes with sterile RB, next irradiating for 200 seconds, followed by 30-second staining with RB, and then a second green light irradiation for 200 seconds. Total fluence was 100 J/cm^2. The cornea was lightly misted periodically with sterile PBS to prevent drying during light exposure. The limbus was shielded from the laser beam by an approximately 11-mm ring placed immediately in front of the cornea. The contralateral eye, which was neither DE- nor RGX-treated, was used as a control.

Clinical Course

The anterior segment of the eyes was evaluated with a surgical microscope (Leica M220 F12; Leica Microsystems, Nussloch, Germany) before and after treatments and at different time points (1, 2, 3, 4, 15, 30, and 60 days, immediately prior to euthanasia). In the clinical follow-up, the epithelial wound was stained by sodium fluorescein (Fluotest; Alcon, Cusi, Barcelona) every day until epithelial closure. Conjunctival hyperemia was quantified from 0 to 4 according to the Efron Scale for hyperemia.[25] Corneal pachymetry was carried out with an ultrasonic pachymeter (Corneo-Gage Plus; Sonogage, Inc., Cleveland, OH, USA).

Tissue Processing and Light Microscopy

Animals were euthanized on days 2, 30, and 60 after treatments by intracardiac injection of sodium pentobarbital (Dolethal 0737-ESP; Vetoquinol, Madrid, Spain) under general anesthesia. Eyes were enucleated and divided into three groups: group 1, DE eyes (DE); group 2, RGX-treated eyes (RGX); and group 3, contralateral untreated eyes (control). They were then fixed with 4% buffered paraformaldehyde and embedded in paraffin. Sections, 5-μm thick were stained with hematoxylin-eosin (H-E). Sections were examined under an Olympus BX41 microscope (Olympus Life Science, Hamburg, Germany) and photomicrographs were obtained with an Olympus DP20 Digital Camera. Quantitative measurements of the photographs were taken using the program Cell A (Olympus Soft Imaging Solutions GmbH, Münster, Germany).

Cell Counting

In each cornea, three measures of corneal full thickness were taken at ×40 magnification. All the H-E stained cells were then counted at ×100 magnification using the Touch Count function from Cell A software (Olympus Soft Imaging Solutions GmbH) in three columns of 90,000 μm^2 (from epithelium to endothelium) in the center of the cornea (wound in DE and RGX) and limbus. Each column was divided into anterior, medial, and posterior layers, each approximately 30,000 μm^2. Layers were 146-μm thick in the control and RGX, and 176-μm thick in DE because of the greater thickness of the DE corneas. All H-E-stained sections were prepared identically to facilitate comparison.

Cell Death: TUNEL Assay

In order to detect DNA fragmentation associated with apoptosis, TUNEL assays were performed in deparaffinized sections following the manufacturer's instructions (TUNEL, G3250; Promega Corp., Madison, WI, USA). Nuclei were counterstained with 4′,6-diamino-2 phenylindole (DAPI; D9542; Sigma-Aldrich, Munich, Germany). TUNEL assay sections were examined with a Leica confocal microscope and Leica Application Suite Advanced software (Leica TSC SP, Wetzlar, Germany). All samples were examined with a ×10 lens.

Cell Proliferation

One hour before euthanasia, the animals received an intramuscular injection of 5-bromo-2′-deoxyuridine (BrdU; Sigma-Aldrich), a DNA synthesis marker (10 mg/mL, 5 mL/kg). Sections were deparaffinized and treated with 2N HCl for 1 hour, then incubated with mouse monoclonal IgG anti-BrdU (DakoCytomation, Carpinteria, CA, USA) for 30 minutes at room temperature. The secondary antibody was fluorescein goat anti-mouse IgG (1:100; Molecular Probes, Leiden, The Netherlands) in Tris-buffered saline. Control sections were prepared by omission of the primary antibody.

Investigative Ophthalmology & Visual Science

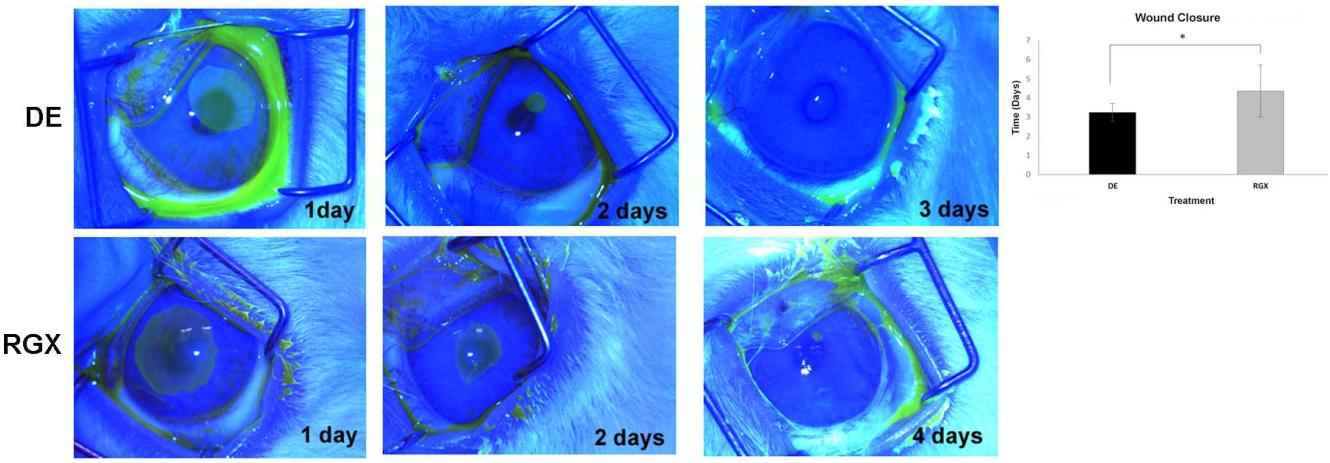

FIGURE 1. Wound closure. Comparison of wound closure time between DE corneas and corneas treated with RGX by fluorescein staining. Graphic of statistical data $^{*}P \leq 0.001$.

Myofibroblastic Differentiation

Myofibroblasts were identified by staining with anti-α-SMA monoclonal antibody (mouse clone 1A4; Dako, Glostrup, Denmark). The secondary antibody was Texas red goat anti-mouse IgG (Molecular Probes). Nuclei were stained with DAPI (Molecular Probes). Limbal blood vessels were used as positive controls, and omission of the primary antibody provided negative controls. Immunofluorescence sections were examined under an Axiophot fluorescence-incorporated microscope (Zeiss Axiophot HB0-50; Carl Zeiss, Oberkochen, Germany) and photomicrographs were captured using the AxioCam HRc Digital Camera and Axiovision release 4.8 software (Carl Zeiss).

Inflammatory Cell Infiltration

Inflammatory cells were labeled with Mac-1 CD11b antibody (NB600-1327; Novus Biologicals Europe, Abingdon, UK). This antigen is present on macrophages, granulocytes, natural killer cells, and blood monocytes. Slides were incubated with monoclonal mouse antibody overnight at room temperature. Primary antibodies were detected by mouse ExtrAvidin Peroxidase Staining Kit antibody produced in goat (Extra2-1KT; Sigma-Aldrich) following the supplier's instructions. A solution of 3,3′-diaminobenzidine (Sigma-Aldrich) was used as a precipitating substrate to locate peroxidase activity.

Statistical Analysis

Variables were analyzed by calculating the mean, SD, coefficient of variation, maximum and minimum values, asymmetry, and coefficient of kurtosis. After defining these parameters, variances were compared using the Levene test. If variances were equal, an ANOVA table was used to test the equality of the means. If the variances were different, then the Kruskal-Wallis test was used to compare the equality of the medians. A multiple range test was also used to determine which means were significantly different from others. Statistical analyses were performed using R program version 3.3.1 (R Core Team 2016. R: A language and environment for statistical computing. R Foundation for Statistical Computing, Vienna, Austria. Available in the public domain, http://www.R-project.org/). *P* values less than 0.05 were considered to be statistically significant.

RESULTS

Clinical Results

Fluorescein testing was positive for 24 hours after treatments and every day until 3.25 ± 0.46 days in DE eyes and at 4.36 ± 1.36 in RGX. This difference between groups was statistically significant (Fig. 1).

There was slight grade 1 ± 0.53-bulbar conjunctival hyperemia in the DE group and 1 ± 0.63 in the RGX group after 24 hours, which then decreased to grade 0 in both groups at the end of follow-up. There were no statistically significant differences between groups at any time (Fig. 2).

After 2 days, all central corneas in the DE group were transparent. After RGX, a slight rose-colored stain of the anterior corneal stroma appeared at day 1 and remained until the end of the study (Fig. 3).

Cornea thickness by pachymetry was measured from presurgery until day 60 and were maximum at day 2, then decreased until day 4, and remained at this level on days 30 and 60. On day 4, the RGX group reached a similar value to that of control, while the DE group maintained the edema and showed statistical differences with the control and RGX groups (Fig. 4).

Corneal Morphology

Hematoxylin-Eosin Sections. After 2 days, in both DE and RGX groups the epithelium did not cover the stroma and was very friable. In both groups, the anterior zone of the stroma was devoid of keratocytes, and some cellular debris could be seen (Figs. 5A, 5B). The endothelium was well preserved and no evidence of edema in the posterior stroma was observed.

After 30 days, the epithelium thickness increased: three or four layers could be observed in DE corneas, while two or three layers were seen in RGX corneas. The corneal stroma in both groups was repopulated with new cells distributed in an irregular arrangement. The endothelium in both groups was similar to that of control eyes (Figs. 5D–F).

At 60 days, the epithelium of DE corneas remained hyperplasic and the stroma was similar to control eyes with a slight edema. Rose bengal–green light crosslinking corneas showed a normal epithelial layer although a subepithelial strip of 27.89 ± 8.04-μm thickness without cells was apparent. The remaining stroma maintained a similar structure to that of controls (Figs. 5G–I).

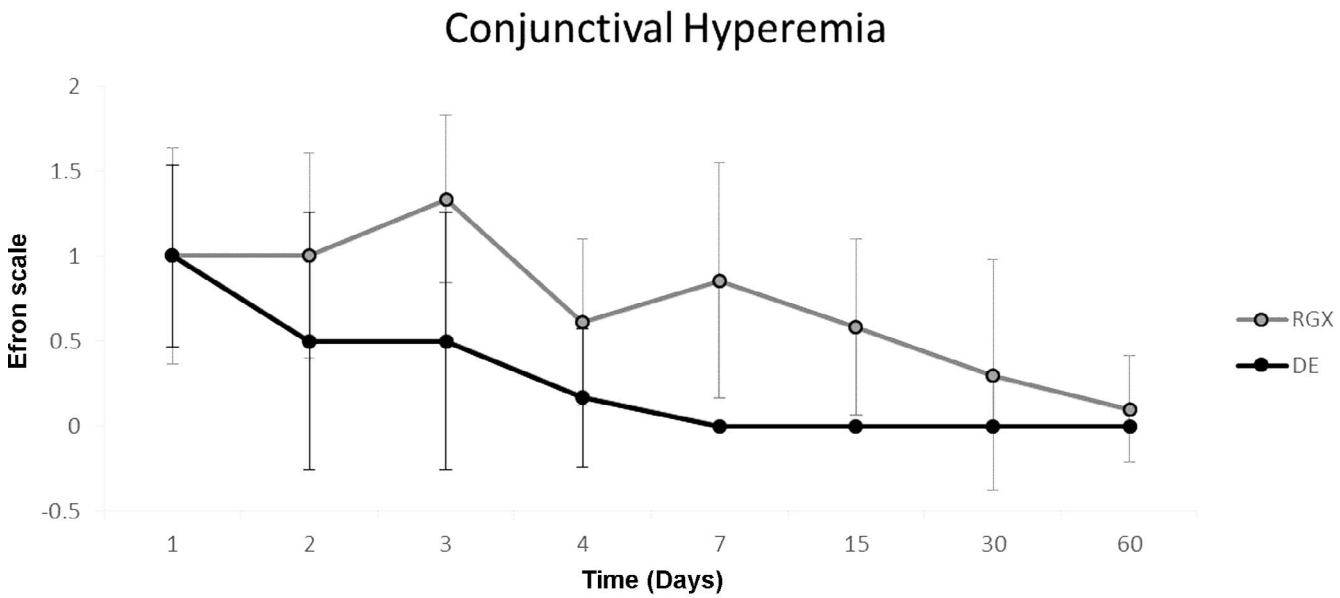

FIGURE 2. Conjunctival hyperemia. Time course of conjunctival hyperemia after DE or treatment with RB as assessed using the Efron Scale for hyperemia.

After 2 days, the conjunctiva displayed a similar epithelium in both groups and an inflammatory hypercellularity, which morphology correspond with neutrophils and was observed in the lamina propria from the RGX corneas. De-epithelialized corneas did not show this characteristic (Fig. 6). These cells are CD 11b positive (Fig. 6 for details). After 1 month, the hypercellularity disappeared in the conjunctiva of RGX-treated eyes.

Corneal Thickness. Corneas from both DE- and RGX-treated eyes showed edema at day 2 that remained in DE corneas until the end of the study. The corneal thickness in the DE corneas was significantly different from that of the RGX and control groups on days 30 and 60. Corneas treated with RGX were slightly thinner than control corneas after 30 and 60 days, but this difference was not statistically significant (Fig. 7).

Epithelial Thickness. After 2 days re-epithelization was greater in DE than in RGX corneas. In RGX corneas, the epithelium was nonexistent or was only a thin layer leading to significant differences in thickness compared with DE corneas. After 30 days, re-epithelization of RGX corneas nearly reached the thickness of control corneas. However, DE corneas showed a hyperplasia that was significantly different compared with the two other groups. At 60 days, the difference between RGX and control was not significant although the DE corneas significantly differed from both the control and RGX corneas (Fig. 8). The epithelial thickness of the area close to the limbus showed no differences in mean values between groups at any point (data not shown).

Cell Population in the Stroma. At day 2, RGX and DE corneas showed prominent losses of keratocytes. The mean number of stromal cells in the center of the wounded corneas showed a significant decrease compared with the control. Although the mean cell number value for RGX was slightly lower than that of DE, the difference of their means was not significant.

Cell recovery was similar after both treatments without reaching the control value at day 30 and day 60. Significant differences with the control were found at 30 and 60 days, although there were no significant differences between the two treatments (Fig. 9A).

The stromal cells in the limbal zone were not affected in either of RGX and DE corneas, because both showed similar cell number cells to that of the control. Oddly, at day 60 the number of stromal cells in RGX-treated corneas had decreased significantly (Fig. 9B).

Because the depth of the damage is very important, we quantified the number of cells per millimeters squared in three areas in the central cornea, namely, anterior, middle, and posterior levels (30,000 μm^2 each), after 2 days as well as cell recovery after 30 and 60 days.

In the anterior area in the central stroma (to a depth of 146 μm in control and RGX, and 176-μm DE), at 2-days post treatment there was major depletion of cells with significant

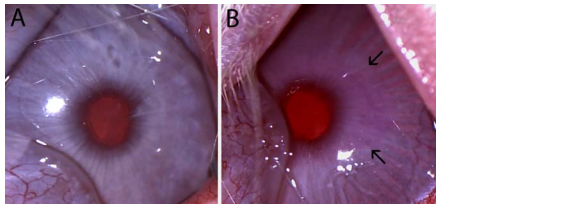

FIGURE 3. Microscopic image showing one DE cornea (**A**) and the characteristic rose staining in RGX group at the end of the study (60 days) (**B**). *Arrows* show limits of pink corneal stain.

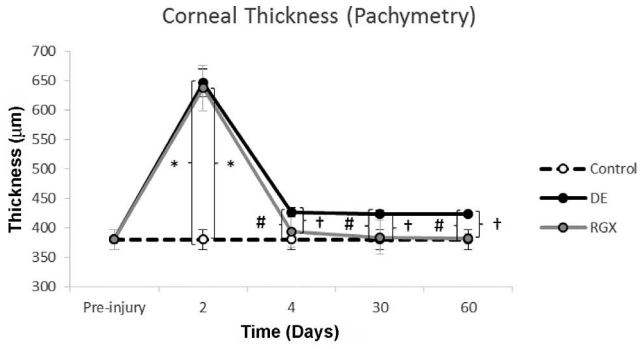

FIGURE 4. Measurements of central cornea thickness using pachymetry from preinjury to 60 days post surgery. *$P \leq 0.001$; #$P \leq 0.01$; †$P \leq 0.05$.

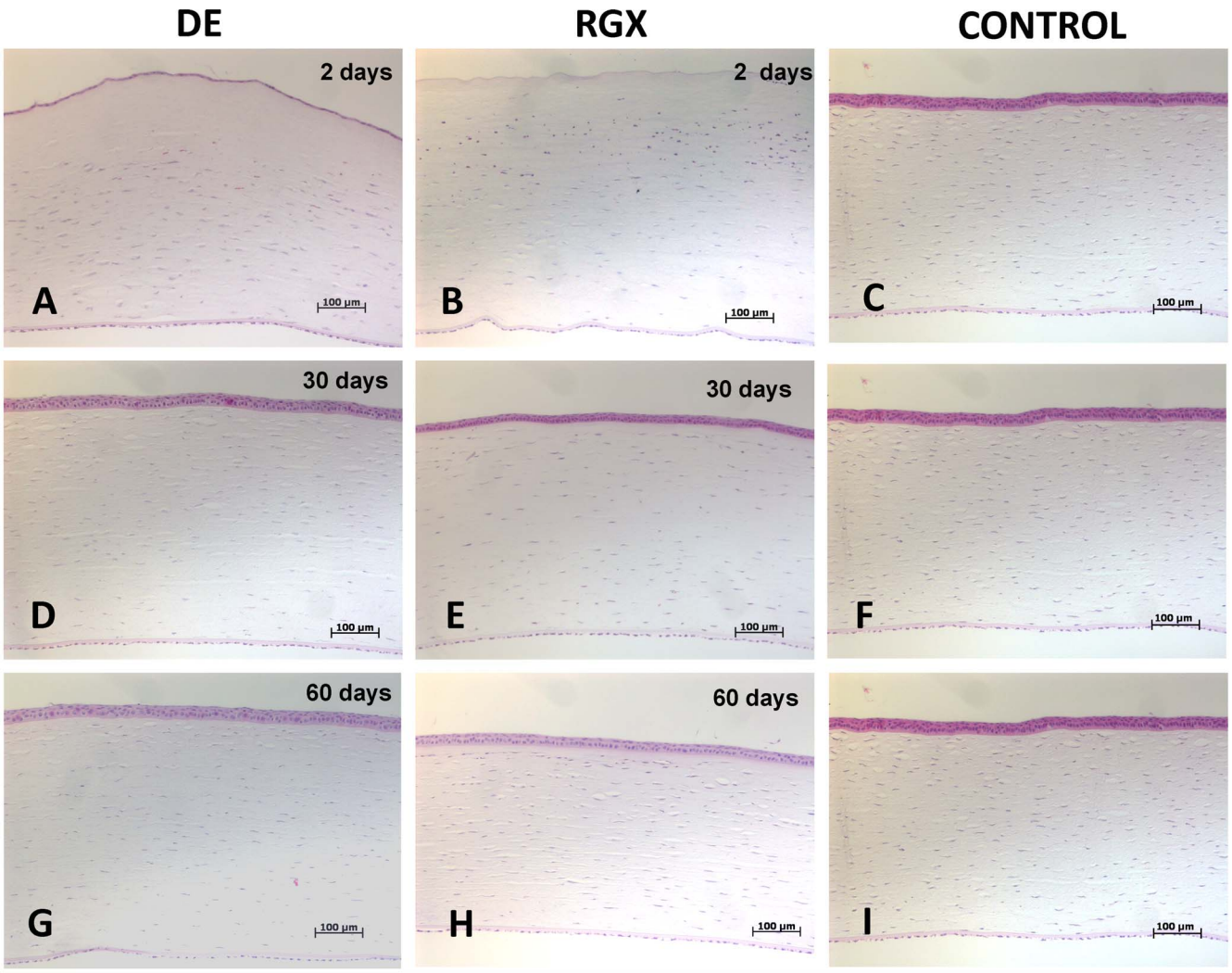

Figure 5. Corneal sections stained with H-E from DE and RGX eyes. (**A**, **B**) Two days post treatment shows cell depletion in both DE- and RGX-treated eyes. (**C**) Untreated control cornea. (**D**, **E**) Thirty days post treatment shows repopulation of keratocytes. (**F**) Untreated control cornea. (**G**, **H**) Sixty days post treatment shows epithelial hyperplasia in DE corneas and regular distribution of keratocytes in both DE and RGX corneas. (**I**) Untreated control cornea.

differences in the number of cells between control and the two treatments as well as between the two treatments (Fig. 10A). At 30 and 60 days after treatment, the cell density of RGX- and DE-treated tissue was partially recovered, showing significant differences with the control, but not between DE and RGX corneas.

In the middle area, there were no significant differences in the mean number of cells or among the groups at the different times analyzed (Fig. 10B).

No differences in the number of cells in the posterior area were observed at 2- and 60-days post treatment between the

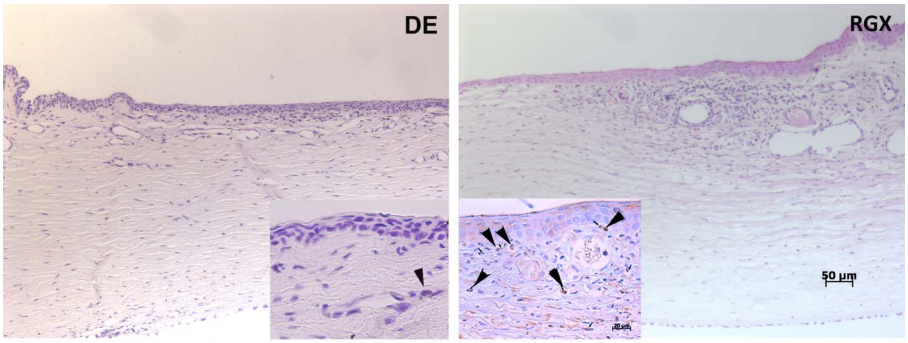

Figure 6. Conjunctival sections stained with hematoxylin from DE and RGX eyes 2 days after treatment, ×100 magnification, *scale bar*: 50 µm. In detail, *arrowheads* indicate inflammatory cells labeled with CD11b antibody, ×400 magnification, *scale bar*: 20 µm.

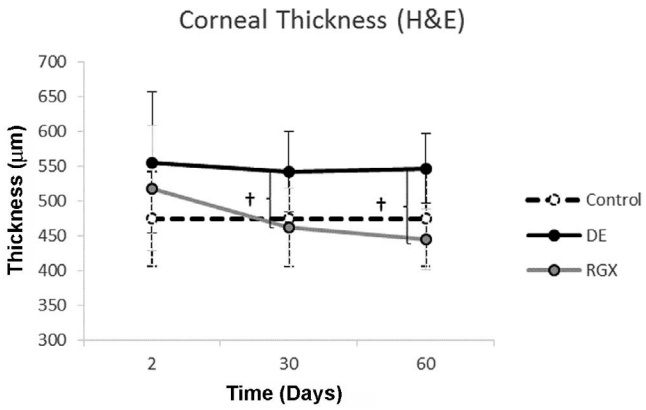

FIGURE 7. Corneal thickness measured on the corneal sections obtained 2, 30, and 60 days post treatment. Sections were stained with H-E. †$P \leq 0.05$.

two treatments and the control (Fig. 10C). However, at day 30, a decrease in the number of cells in DE corneas was observed compared with the control, as well as an increase in the number of cells in RGX corneas, leading to significant differences between DE and RGX.

Cell Death

Two days after RGX or DE, cells showed labeling with the TUNEL technique in the anterior stroma (Fig. 11). This area coincided with the area scraped to remove the epithelium. The appearance of the fluorescent label differed between DE and RGX. De-epithelialized corneas showed chromatin fragmentation with membrane bound structures, suggesting apoptotic bodies, which are visualized by faint fluorescence. Rose bengal–green light crosslinking corneas showed cell shrinkage and chromatin condensation that is visualized as strong fluorescence. This difference indicates that apoptosis occurred in DE corneas with a slightly different time course than in RGX corneas. At day 30, some scattered labeled cells were seen in the middle stroma. At day 60, no labeled cells were found.

No endothelial TUNEL-positive cells appeared. Some labeled cells were observed on the surface of the epithelium and in the lamina propria of conjunctiva. No TUNEL-positive cells were observed in the iris or retina.

Cell Proliferation

At day 2 after de-epithelialization or RGX treatment, proliferation of the epithelium, as detected by BrdU labeling, was located in the limbus (Figs. 12C, 12F) as well as in the recently formed epithelium in the intermediate area (Figs. 12B, 12E) and close to the wound (Figs. 12A, 12D). Fibroblast proliferation started below the epithelium. No BrdU-positive cells were seen at this time in the posterior stroma and no BrdU-positive cells were observed on day 30 or 60.

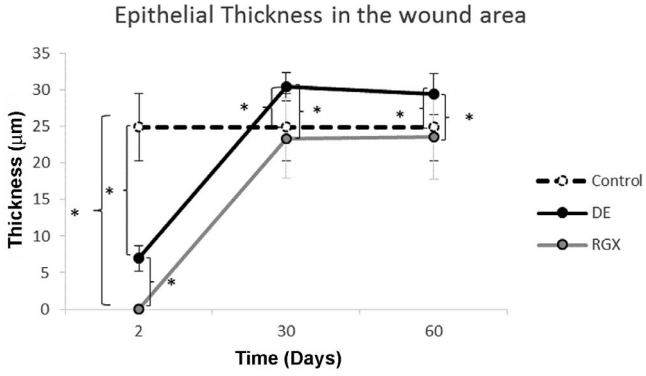

FIGURE 8. Epithelial thickness evolution after DE and RGX treatments. *$P \leq 0.001$.

Myofibroblast Differentiation

No α-SMA–positive cells (myofibroblasts) were observed at either 30 or 60 days in RGX or DE corneas. The artery walls in the limbus were used as positive controls for α-SMA immunohistochemistry.

Discussion

The results of this study indicate that major aspects of cornea wound healing after RGX treatment were the same or very similar to those occurring after DE alone. These aspects include, for stromal healing, the kinetics and magnitude of cell repopulation below the wound over the 60-day healing period, stromal cell death by apoptosis, and the absence of myofibroblast development. However, DE corneas remained edematous for 60 days, whereas RGX-treated corneas returned to normal more rapidly and RGX produced a narrow anterior strip of cell-free stroma that was absent after DE only. For epithelial healing, wound closure on RGX-treated corneas was only modestly delayed compared with DE corneas and healing produced a normal epithelium in RGX corneas compared with a hyperplastic epithelium after DE only.

This study took the approach of comparing healing processes after RGX treatment with that after DE alone in order to allow any additional effects RGX to be identified. We have also compared, in this discussion, our results with the extensive literature reports of healing after the currently used treatment, conventional CXL.[26–29]

During clinical follow-up, edema measured by pachymetry increased rapidly after treatment with both RGX and DE, although at day 4 the RGX-treated corneas recovered to values close to the control values, whereas DE corneas displayed a significant increase that remained throughout the 60-day study (Fig. 4). In conventional CXL, the edema was described as being clinically high for up to 7 days in an experimental rabbit model[28] and high up to 2 weeks using high-definition optical coherence tomography, ultrasound and dual Scheinmplug tomography in humans due to transient mild endothelial decompensation.[30,31] However, 2 months later, corneas had no edema at slit-lamp in a rabbit eye study.[26] Corneal thickness measured on H-E sections also showed continued thickening in DE corneas for up to 2 months, while RGX led to cornea slimming (Fig. 6), similar to the thinner corneas reported by Wollensak and Iomdina[32] after conventional riboflavin CXL.

Clinical inflammatory signs of hyperemia were noticeable in RGX corneas, which is consistent with vessel injection and inflammatory infiltrates. In conventional CXL, no increase in vessel injection and no inflammatory infiltrates were reported.[33]

A light pink color remained in the stroma of RGX-treated corneas until the end of the experiment (Fig. 3), which was faint compared with the color prior to irradiation. Interestingly, this color is not visible when RB is used to stain corneal ulcers or filaments of mucus in dry eye and other corneal diseases,[34–36] likely because the epithelial mucin layer does not allow penetration of this dye through the epithelium to the stroma where it associates strongly with collagen.

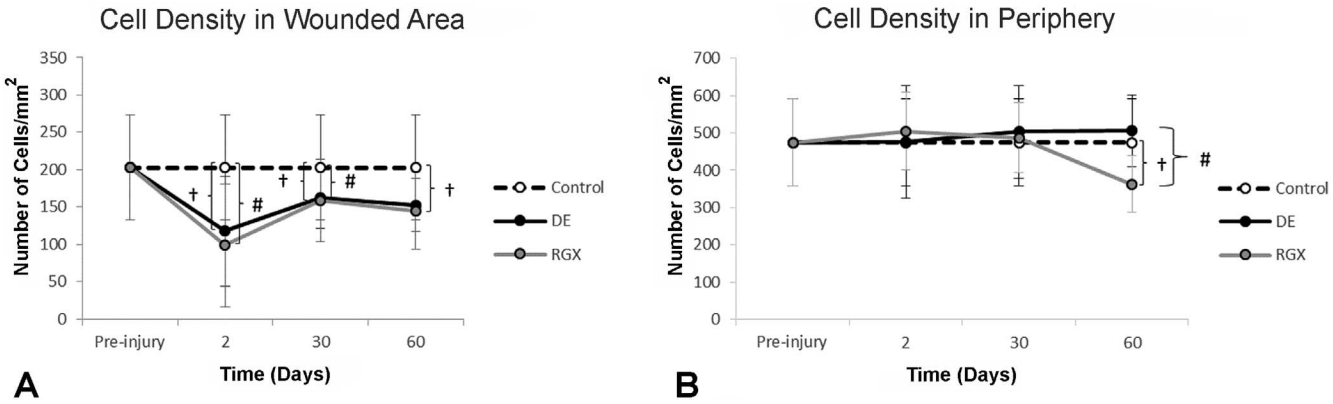

FIGURE 9. Total cell number in the stroma of DE- and RGX-treated corneas in (**A**) the wounded central corneal and in (**B**) the untreated limbal area as a function of time after treatment. $^{*}P \leq 0.001$; $\#P \leq 0.01$; $\dagger P \leq 0.05$.

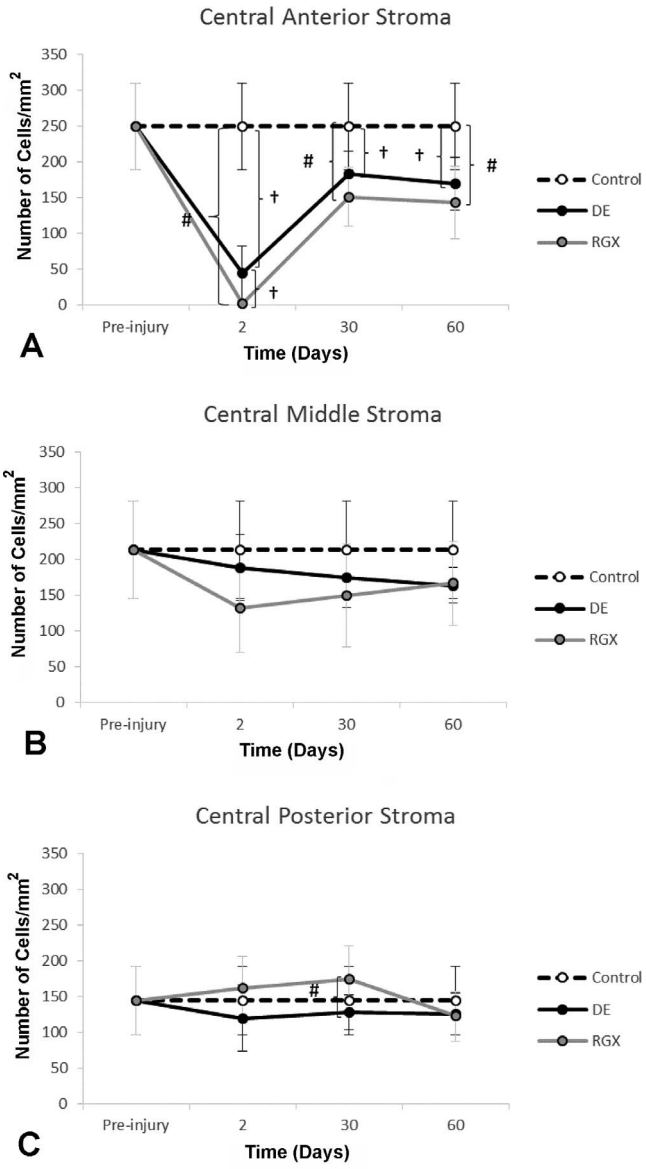

FIGURE 10. Number of cells in the central cornea, where the wound was localized, in bands at varying depths in the stroma and at varying times pre- and posttreatment. (**A**) Anterior one-third of the stroma, (**B**) middle one-third, (**C**) and posterior one-third. $^{*}P \leq 0.001$; $\#P \leq 0.01$; $\dagger P \leq 0.05$.

Other similarities between healing of RGX- and DE-treated corneas were found by histology. The first stromal event in the wound healing process, apoptosis, and loss of keratocytes,[37] showed little difference between DE and RGX corneas. Previous studies have described apoptosis after conventional CXL,[26–29,38] and Wilson and Moller-Pedersen[39,40] have described it in DE corneas, although study times differed substantially. We chose 2 days for our study because at this time point, in our experience,[41,42] apoptosis and proliferation coincide. We were thus able to minimize the number of animals for the study. The TUNEL assay after RGX and DE showed limited cell damage localized in the anterior central area of the stroma similar to the results obtained by Wilson et al.,[40] in a study of epithelial debridement. In contrast, highly variable results have been reported for apoptosis after conventional CXL from apoptosis throughout the whole stroma including the endothelium,[26,28] to means of 38.7 cells/×400 TUNEL-positive cells[27] or 200 TUNEL-positive cells/×400[26] without reference to depth. Esquenazi et al.[38] localized apoptosis in the anterior 250 μm of the stroma.

Cell death produced a zone depleted of keratocytes in the anterior portion of the stroma as shown in Figures 5A, 5B, 10A, and 10B. The total number of keratocytes in the central cornea on day 2 showed a decrease, with no difference between RGX and DE (Fig. 9A) although the decrease on day 2 in the anterior area (~146 μm) of the cornea was significantly greater for RGX than for DE (Fig. 10A), consistent with a prior report.[23] Rose bengal has been shown to diffuse only approximately 120 μm into the DE stroma and, consequently, would affect the cells mainly in this region.[22]

The second event in the wound healing process is regeneration of the damaged cornea. First, the epithelium and then the stroma must be repopulated. Two biological events are required for this, namely, proliferation and migration of activated cells. Epithelial regeneration requires the integrity of limbal stem cells and for this reason we protected the limbus. As shown in Figure 12C, the limbal stem cells were BrdU (a proliferative marker) positive. However, as mentioned above, the migration of epithelial cells was slower in RGX than in DE corneas. The reason for this is not clear. However, the epithelium thickness recovers after RGX until nearly control values at day 60. On days 30 and 60, DE corneas displayed hyperplasia (Fig. 8) as described in Wilson et al.[37] in healing after photorefractive keratectomy.

Stromal cell proliferation commenced 2 days after either RGX or DE as shown by the BrdU-labeled cells in the stroma (Figs. 12B, 12E). Stromal repopulation was rapid during the first 30 days, although not enough to reach the control number even after 60 days in both RGX and DE corneas. Our

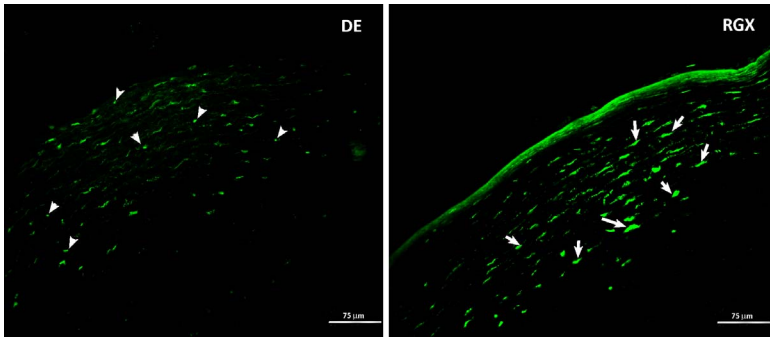

FIGURE 11. Cell death in corneas 2 days after DE (*arrowheads* point to apoptotic bodies) or RGX (*arrows* show bright cells in condensated nuclei) as assessed by the TUNEL assay.

previous study had shown that repopulation was the same after both RGX and DE, although no comparison was made to eyes that had not been DE.[23] Using conventional CXL treatment, at 6-weeks[28,43] and 2-months[26] post treatment, the number of stromal cells had fully recovered, although Esquenazi et al.[38] observed migration of activated keratocytes 10 weeks after conventional CXL treatment. When studying DE by confocal microscopy, Moller-Pedersen et al.[39] described images similar to pretreatment patterns of images 3 months later. In patients, confocal microscopy has shown a significant reduction in anterior keratocyte density, compared with preoperative values, 12 months later.[44] It is therefore possible that a long process is needed to reach pretreatment cell number.

Simultaneous with proliferation, activated stromal cells migrate into the cell-depleted stroma. With green light energy, RB applied to the stroma leads to chemical bonds between collagen molecules or other stromal macromolecules.[23] These junctions between collagen and macromolecules in the extracellular matrix could slow down keratocyte migration and cell repopulation in the approximately 25- to 30-µm cell-depleted strip at the anterior surface that was observed on histology (Fig. 5F).

Finally, neither DE nor RGX showed myofibroblast differentiation as no α-SMA–positive cells were found at any time in our study. This observation contrasts with the results reported for conventional CXL.[26,27,38]

Increased corneal stiffness after RGX was initially established in ex vivo studies using extension tensiometry and Scheimpflug air puff corneal deformation imaging. More recently, increased stiffness after in vivo treatment has been shown to remain for 1[23] and 2 months.[24] In addition, the deformation parameters of RGX corneas have been shown to be lower than those of the control and even after conventional CXL because of the greater effect of RGX on the anterior approximately 120 µm of stroma where RB localizes.[24] These results indicate that, despite wound healing involving cell proliferation, cell migration, and remodeling of the extracellular matrix, the bonds established between the collagen fibers by RGX are robust.

Taken together, the results of this study indicating very similar healing processes after RGX compared with DE alone, the results of a previous study indicating that the RGX treatment conditions do not cause retinal damage[23] and the ability of RGX to stiffen corneas by CXL only near the anterior surface[22–24] suggest that RGX may be a good treatment for

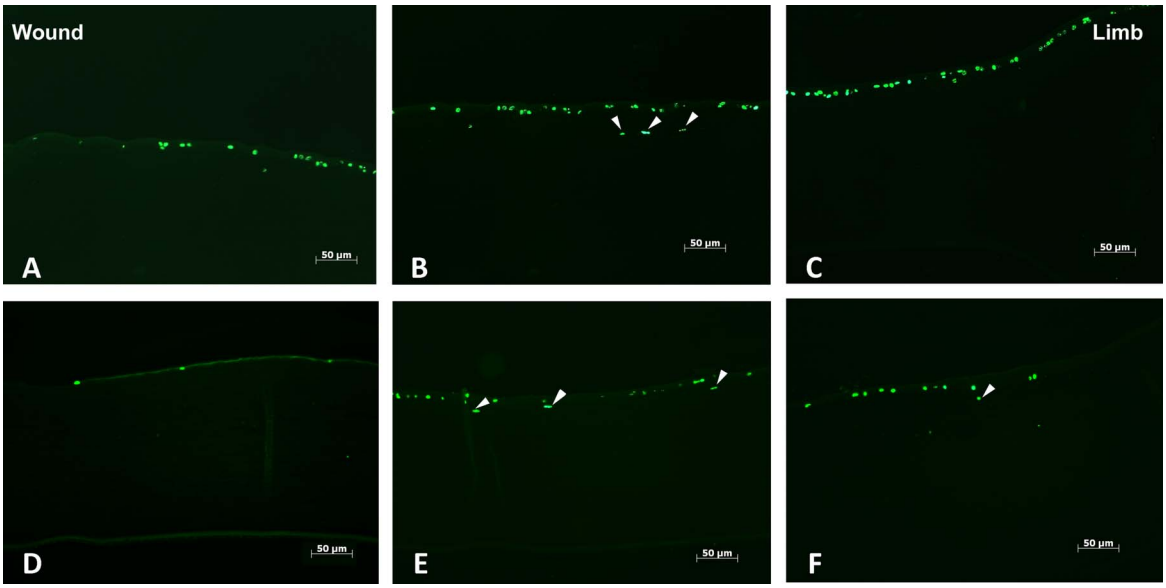

FIGURE 12. Cell proliferation detected by BrdU labeling 2 days after DE (**A**–**C**) or RGX (**D**–**F**). (**A**, **D**) Sections taken from the region close to the wound. (**B**, **E**) Sections taken from the area between the wound and the limbus. *Arrows* point to BrdU positive fibroblasts. (**C**, **F**) Sections from the limbal zone.

Investigative Ophthalmology & Visual Science

advanced stage keratoconus and post-LASIK ectasias, particularly of those eyes with thin corneas.

Acknowledgments

The authors thank Cristina Herrero Pérez for her technical assistance; Sagrario Callejo for her technical assistance with the confocal images; and Maria Cruz Valsero and Itziar Fernández for statistical analysis.

Disclosure: **P. Gallego-Muñoz**, None; **L. Ibares-Frías**, None; **E. Lorenzo**, None; **S. Marcos**, None; **P. Peréz-Merino**, None; **N. Bekesi**, None; **I.E. Kochevar**, None; **M.C. Martínez-García**, None

References

1. Wollensak G. Crosslinking treatment of progressive keratoconus: new hope. *Curr Opin Ophthalmol*. 2006;17:356–360.
2. Spadea L. Corneal collagen crosslinking with riboflavin and UVA irradiation in pellucid marginal degeneration. *J Refract Surg*. 2010;26:375–377.
3. Bekesi N, Kochevar IE, Marcos S. Corneal biomechanical response following collagen crosslinking with rose bengal-green light and riboflavin-UVA. *Invest Ophthalmol Vis Sci*. 2016;57:992–1001.
4. Zhang Y, Conrad AH, Conrad GW. Effects of ultraviolet-A and riboflavin on the interaction of collagen and proteoglycans during corneal crosslinking. *J Biol Chem*. 2011;286:13011–13022.
5. Kamaev P, Friedman MD, Sherr E, Muller D. Photochemical kinetics of corneal crosslinking with riboflavin. *Invest Ophthalmol Vis Sci*. 2012;53:2360–2367.
6. Wollensak G, Spoerl E, Seiler T. Stress-strain measurements of human and porcine corneas after riboflavin-ultraviolet-A-induced crosslinking. *J Cataract Refract Surg*. 2003;29:1780–1785.
7. Spoerl E, Wollensak G, Seiler T. Increased resistance of crosslinked cornea against enzymatic digestion. *Curr Eye Res*. 2004;29:35–40.
8. Spoerl E, Wollensak G, Dittert DD, Seiler T. Thermomechanical behavior of collagen-cross-linked porcine cornea. *Ophthalmologica*. 2004;218:136–140.
9. Kymionis GD, Portaliou DM, Diakonis VF, Kounis GA, Panagopoulou SI, Grentzelos MA. Corneal collagen crosslinking with riboflavin and ultraviolet-A irradiation in patients with thin corneas. *Am J Ophthalmol*. 2012;153:24–28.
10. Chatzis N, Hafezi F. Progression of keratoconus and efficacy of pediatric [corrected] corneal collagen crosslinking in children and adolescents. *J Refract Surg*. 2013;28:753–758.
11. Goldich Y, Barkana Y, Wussuku Lior O, et al. Corneal collagen crosslinking for the treatment of progressive keratoconus: 3-year prospective outcome. *Can J Ophthalmol*. 2014;49:54–59.
12. Hafezi F. Limitation of collagen crosslinking with hypoosmolar riboflavin solution: failure in an extremely thin cornea. *Cornea*. 2011;30:917–919.
13. Caporossi A, Mazzotta C, Paradiso AL, Baiocchi S, Marigliani D, Caporossi T. Transepithelial corneal collagen crosslinking for progressive keratoconus: 24-month clinical results. *J Cataract Refract Surg*. 2013;39:1157–1163.
14. Filippello M, Stagni E, Buccoliero D, Bonfiglio V, Avitabile T. Transepithelial crosslinking in keratoconus patients: confocal analysis. *Optom Vis Sci*. 2012;89:e1–e7.
15. Bouheraoua N, Jouve L, Borderie V, Laroche L. Three different protocols of corneal collagen crosslinking in keratoconus: conventional, accelerated and iontophoresis. *J Vis Exp*. 2015;105.
16. Hashemi H, Miraftab M, Seyedian MA, et al. Long-term results of an accelerated corneal crosslinking protocol (18 mW/cm2) for the treatment of progressive keratoconus. *Am J Ophthalmol*. 2015;160:1164–1170.e1.
17. Shetty R, Matalia H, Nuijts R, et al. Safety profile of accelerated corneal crosslinking versus conventional crosslinking: a comparative study on ex vivo-cultured limbal epithelial cells. *Br J Ophthalmol*. 2015;99:272–280.
18. Mandathara PS, Stapleton FJ, Willcox MD. Outcome of keratoconus management: review of the past 20 years' contemporary treatment modalities. *Eye Contact Lens*. 2017;43:141–154.
19. Proano CE, Azar DT, Mocan MC, Redmond RW, Kochevar IE. Photochemical keratodesmos as an adjunct to sutures for bonding penetrating keratoplasty corneal incisions. *J Cataract Refract Surg*. 2004;30:2420–2424.
20. Verter EE, Gisel TE, Yang P, Johnson AJ, Redmond RW, Kochevar IE. Light-initiated bonding of amniotic membrane to cornea. *Invest Ophthalmol Vis Sci*. 2011;52:9470–9477.
21. Tsao S, Yao M, Tsao H, et al. Light-activated tissue bonding for excisional wound closure: a split-lesion clinical trial. *Br J Dermatol*. 2012;166:555–563.
22. Cherfan D, Verter EE, Melki S, et al. Collagen crosslinking using rose bengal and green light to increase corneal stiffness. *Invest Ophthalmol Vis Sci*. 2013;54:3426–3433.
23. Zhu H, Alt C, Webb RH, Melki S, Kochevar IE. Corneal crosslinking with rose bengal and green light: efficacy and safety evaluation. *Cornea*. 2016;35:1234–1241.
24. Bekesi N, Gallego-Munoz P, Ibares-Frias L, et al. Biomechanical changes after in vivo collagen crosslinking with rose bengal-green light and riboflavin-UVA. *Invest Ophthalmol Vis Sci*. 2017;58:1612–1620.
25. Efron N, Morgan PB, Katsara SS. Validation of grading scales for contact lens complications. *Ophthalmic Physiol Opt*. 2001;21:17–29.
26. Armstrong BK, Lin MP, Ford MR, et al. Biological and biomechanical responses to traditional epithelium-off and transepithelial riboflavin-UVA CXL techniques in rabbits. *J Refract Surg*. 2013;29:332–341.
27. Salomao MQ, Chaurasia SS, Sinha-Roy A, et al. Corneal wound healing after ultraviolet-A/riboflavin collagen crosslinking: a rabbit study. *J Refract Surg*. 2011;27:401–407.
28. Wollensak G, Iomdina E, Dittert DD, Herbst H. Wound healing in the rabbit cornea after corneal collagen crosslinking with riboflavin and UVA. *Cornea*. 2007;26:600–605.
29. Wollensak G, Spoerl E, Wilsch M, Seiler T. Keratocyte apoptosis after corneal collagen crosslinking using riboflavin/UVA treatment. *Cornea*. 2004;23:43–49.
30. Antonios R, Fattah MA, Maalouf F, Abiad B, Awwad ST. Central corneal thickness after crosslinking using high-definition optical coherence tomography, ultrasound, and dual Scheimpflug tomography: a comparative study over one year. *Am J Ophthalmol*. 2016;167:38–47.
31. Baiocchi S, Mazzotta C, Cerretani D, Caporossi T, Caporossi A. Corneal crosslinking: riboflavin concentration in corneal stroma exposed with and without epithelium. *J Cataract Refract Surg*. 2009;35:893–899.
32. Wollensak G, Iomdina E. Long-term biomechanical properties of rabbit cornea after photodynamic collagen crosslinking. *Acta Ophthalmol*. 2009;87:48–51.
33. Wollensak G, Mazzotta C, Kalinski T, Sel S. Limbal and conjunctival epithelium after corneal crosslinking using riboflavin and UVA. *Cornea*. 2011;30:1448–1454.
34. Doughty MJ. Rose bengal staining as an assessment of ocular surface damage and recovery in dry eye disease-a review. *Cont Lens Anterior Eye*. 2013;36:272–280.

35. Efron N. Putting vital stains in context. *Clin Exp Optom*. 2013;96:400–421.
36. Argueso P, Tisdale A, Spurr-Michaud S, Sumiyoshi M, Gipson IK. Mucin characteristics of human corneal-limbal epithelial cells that exclude the rose bengal anionic dye. *Invest Ophthalmol Vis Sci*. 2006;47:113–119.
37. Wilson SE, Mohan RR, Mohan RR, Ambrosio R Jr, Hong J, Lee J. The corneal wound healing response: cytokine-mediated interaction of the epithelium, stroma, and inflammatory cells. *Prog Retin Eye Res*. 2001;20:625–637.
38. Esquenazi S, He J, Li N, Bazan HE. Immunofluorescence of rabbit corneas after collagen crosslinking treatment with riboflavin and ultraviolet A. *Cornea*. 2010;29:412–417.
39. Moller-Pedersen T, Cavanagh HD, Petroll WM, Jester JV. Corneal haze development after PRK is regulated by volume of stromal tissue removal. *Cornea*. 1998;17:627–639.
40. Wilson SE, He YG, Weng J, et al. Epithelial injury induces keratocyte apoptosis: hypothesized role for the interleukin-1 system in the modulation of corneal tissue organization and wound healing. *Exp Eye Res*. 1996;62:325–327.
41. Ibares-Frias L, Gallego P, Cantalapiedra-Rodriguez R, et al. Tissue reaction after intrastromal corneal ring implantation in an experimental animal model. *Graefes Arch Clin Exp Ophthalmol*. 2015;253:1071–1083.
42. Martinez-Garcia MC, Merayo-Lloves J, Blanco-Mezquita T, Mar-Sardana S. Wound healing following refractive surgery in hens. *Exp Eye Res*. 2006;83:728–735.
43. Kruger A, Hovakimyan M, Ramirez Ojeda DF, et al. Combined nonlinear and femtosecond confocal laser-scanning microscopy of rabbit corneas after photochemical crosslinking. *Invest Ophthalmol Vis Sci*. 2011;52:4247–4255.
44. Mastropasqua L, Nubile M, Lanzini M, et al. Morphological modification of the cornea after standard and transepithelial corneal crosslinking as imaged by anterior segment optical coherence tomography and laser scanning in vivo confocal microscopy. *Cornea*. 2013;32:855–861.

Investigative Ophthalmology & Visual Science